COMBINED HYDROGEN, HEAT AND ELECTRICITY VIA BIOGAS REFORMING: ENERGY AND ECONOMIC ASSESSMENTS

Mariagiovanna Minutillo[a], Alessandra Perna[b], Alessandro Sorce[c]

[a]Department of Engineering, University of Naples "Parthenope", Naples, Italy

[b]Department of Civil and Mechanical Engineering, University of Cassino and Southern Lazio, Cassino, Italy

[c]Department of Mechanical, Energy, Management and Transportation Engineering, University of Genova, Genova, Italy

Abstract

Energy systems designed for providing multiple energy services like hydrogen, heating, electricity represent a possible sustainable energy solution for the transition to low-carbon future energy systems thanks to a substantial increase in overall efficiency. A further step to reach zero-carbon energy systems can be done by using renewables as primary sources.

In this study a biomass-based Multi-Energy System (MES) for the combined hydrogen, heat and electricity is designed and analyzed from energy and economic points of view. By means of an anaerobic digester, the biomass is converted in biogas that is used to feed a polygeneration system consisting of a fuel processing unit, an SOFC (Solid Oxide Fuel Cell) power unit and a hydrogen separation and storage unit.

The energy analysis has been investigated by using the numerical simulation based on thermo-electrochemical models. Four operating conditions, related to different SOFC loads (from 30% to 100%), have been analyzed. The calculated overall efficiencies range from 68.5% (80% SOFC load) to 72.3% (30% SOFC load) and the energy saving, obtained with respect to the separate production of hydrogen, heat and electricity, ranges from about 8% to 26%.

The economic assessment carried out by evaluating the total capital investment and the plant profitability has been carried out by analyzing different management strategies (base load, peaker, ancillary and mobility) that account for different technological development and market scenarios. Results show that the hydrogen production is the main contributor to the MES economic sustainability and the use of the MES within a Virtual Power Plant for increasing the grid resilience, is less convenient in comparison to the MES managed for the hydrogen production (Mobility options) thanks to the highest prices of hydrogen with respect to the electricity ones.

K**eywords:** Biogas, Hydrogen, SOFC, Multi-Energy system, Virtual Power Plant, Economic Indicators

NOMENCLATURE

A/B	Air to Biogas ratio (kg/kg)
AR	Annual Revenue (k€)
ASR	Area Specific Resistance (Ω cm^2)
ATR	Autothermal Reforming Reactor
C	Compressor
CB	Catalytic burner
CCHP	Combined cooling, heating and electric power
CHP	Combined heat and power
f_{stack}	stack loss factor
j_{cell}	Cell Current density (A/cm^2)
FIT	Feed in Tariff
GHG	Greenhouse Gas

HE	Heat Exchanger
HRF	Hydrogen recovery factor
IC	Ionic compressor
LHV	Lower Heating Value (MJ/kg)
MES	Multi-Energy System
OCV	Open Circuit Voltage (V)
P_W	Electrical Market price (€/kWh)
P_Q	Thermal Power price (€/kWh)
$P_{\Phi_{H2}}$	Chemical power of the product hydrogen price (€/kWh)
Pd-M	Palladium Membrane
Q	Thermal power (kW)
S/B	Steam to Biogas ratio (kg/kg)
SEP	Separation unit
TDS	Technological Development Scenarios
V_{stack}	Stack Voltage (V)
V_{nom}	Nominal cell voltage (V)
W	Electric power (kW)
WGSR	Water Gas Shift Reactor
Φ_{H2}	Chemical power of the product hydrogen (kW)
Φ_{Biogas}	Chemical power of the biogas (kW)
η_{CFP}	Overall efficiency in the co-production of fuel and power (%)
η_{el}	Electrical efficiency (%)
η_{th}	Thermal efficiency (%)
η_{H2}	Hydrogen production efficiency (%)

$\eta_{el,ref}$	Electrical efficiency of a reference technology (%)
$\eta_{th,ref}$	Thermal efficiency of a reference technology (%)
$\eta_{H2,ref}$	Hydrogen production efficiency of a reference technology (%)
Subscrpits	
h	Hours
Peak	peak periods
Off-Peak	off-peak periods
AS up	Ancillary Service, off- peak periods, with low grid generation
AS down	Ancillary Service, peak periods, with high grid generation

1. Introduction

Polygeneration is considered as a possible sustainable energy solution for the transition to low-carbon and zero-carbon future energy systems that interconnect electricity, thermal energy and fuel demands for transportation sector all together. Overall efficiency increases significantly if the system design and integration of sub-systems are done efficiently and thus, also the reduction of pollution and greenhouse gas emissions is achieved [1].

Energy systems based on the concept of polygeneration can use multiple energy sources (renewable and non-renewable), providing multiple energy services (heating, cooling, electricity) and other products (water, hydrogen, etc.) [2-10].

Polygeneration systems can be classified from different perspectives: i) systems using local resources for small and large-scale generation [4-6]; ii) hybrid systems with multiple types of inputs including both fossil and renewable [7]; iii) systems with multiple types of energy services and other useful outputs (i.e. electricity, heating, cooling, clean fuels, potable water, etc.) [8,9].

Ghaem et al. [4] studied the optimal solution of a CHP (combined heat and power) system for

residential applications, based on solar (PV) or wind source, considering three operating strategies (following thermal load, following electric load and modified base load) by using a multi-dimensional objective function. All the operating strategies demonstrated considerable energy, economic and environmental benefits.

In [5] the technical and economical performances of a small scale trigeneration power plant, based on solid oxide fuel cells and designed for a small residential cluster, is presented. The energy system features a natural gas solid oxide fuel cell, a boiler, a refrigerator, and a thermal storage system.

Rivarolo et al. [6] presented an original hierarchical approach for the thermo-economic analysis of polygeneration energy systems (cogenerative and trigenerative configurations) in time dependent conditions. The aim of the study was the optimization of both the size and the management of the plant components installed in an energy district, analyzing different configurations.

In [7] a novel multigeneration system (heating, cooling, electricity, hydrogen, water) fed by biogas-geothermal heat source is proposed and simulated. To demonstrate the feasibility of the proposed multigeneration system, first and second laws analysis are employed as the most effective tools for the performance assessment.

Spencer et al. [8] studied and designed a combined heat, hydrogen and power plant for waste-to-energy conversion. The plant was centered on a Molten Carbonate Fuel Cell (Fuel Cell Energy DFC-1500) fueled by the syngas produced in a municipal waste gasifier. An internal reforming was used to convert the excess fuel from the anode off-gas to an H_2-rich stream. The hydrogen, purified downstream in a pressure-swing adsorption system, was then compressed and stored for refueling PEM fuel cell buses. The authors also performed an economic analysis that highlighted the needed of incentives for the economic profitability of the plant according to the estimated operating costs.

Perna et al. [9] designed a small-scale combined heat, hydrogen and power (CHHP) system that used ammonia as primary energy source. The plant was organized in a power production section, a hydrogen separation section and a hydrogen compression and storage section. The core of the plant was a SOFC module where the ammonia decomposition occurred, and electrical power was generated at low fuel utilization factor. The excess hydrogen from the anode off-gas was compressed (820 bars) and stored for a refueling station. Results highlighted that the efficiency in the co-production of heat, hydrogen and electricity was higher than 70%. Great interest has been also devoted to the biorefineries as polygeneration systems. They can be defined as a facility that integrates conversion processes and equipment to produce fuels, power and chemicals from biomass [11]; in fact, in biorefineries a range of products are obtained and several fundamental process steps (pre-treatment, conversion and downstream processes) are integrated. Thus, these plants, above all if integrated with high efficiency fuel cell systems, can be considered the backbone of the future production of sustainable energy outputs [12].

Several biofuels supply chains, such as the bio-methane chain (both gaseous and liquid), the bio-hydrogen chain, the methanol chain and the butanol chain are considered of strategic interest for a sustainable development [13,14] in transport and chemical industry applications. In particular, the hydrogen produced by renewable sources (wind, biomass, etc.) is considered the most attractive and clean fuel for the novel model of a sustainable mobility based on fuel cell vehicles and, thus, its production is widely studied [15,16].

Therefore, in this contest, focused on the bio-hydrogen production chain and on the hydrogen utilization technologies, the authors propose a detailed energy and economic analysis of an SOFC-based polygeneration system for the combined hydrogen, heat and electricity production by using biogas as primary source [17].

Moreover, the proposed polygeneration system has also been designed with the idea to represent

an alternative solution for the operation of existing biogas power plants (based on anaerobic digestion process) that, by means of the hydrogen production, can increase their flexibility, enabling the economical sustainability in the near future when incentives in the electric power production will no longer be available (in the European market several subMW biogas power plant were built supported by a Feed in Tariff incentives scheme) [18].

Figure 1 shows the concept of the biofuel-based Multi-Energy System (MES) that is designed and managed for the combined hydrogen, heat and electricity production by using biomass as primary energy source.

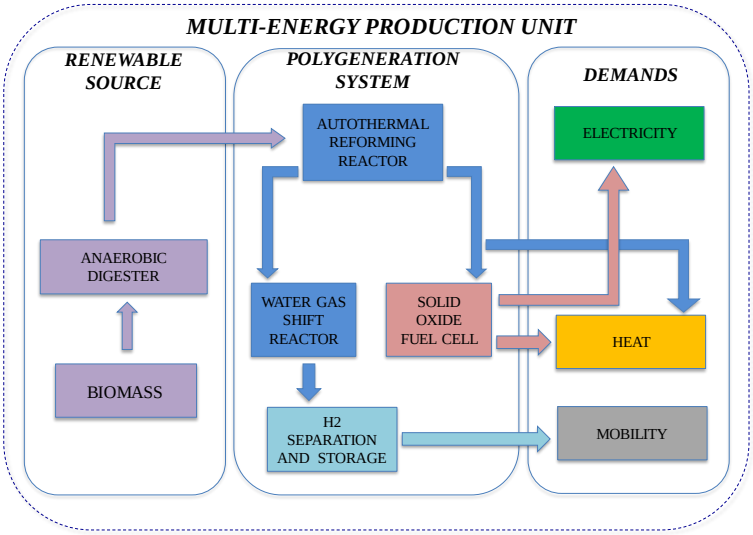

Figure 1. Conceptual scheme of the biomass-based MES

By converting the biomass in an anaerobic digester, the produced biogas is used to feed the polygeneration system that consists of: i) a biogas processing unit, based on autothermal reforming technology, in which a hydrogen-rich gas is generated, ii) a power unit based on SOFC technology, iii) a hydrogen separation unit based on membrane technology and iv) a hydrogen compression and storage unit based on ionic compressor technology.

The energy analysis is conducted by means of the numerical simulation based on thermo-electrochemical models. In order to valorize the electricity and/or the hydrogen production, different plant operating modes, obtained by working the SOFC power unit at partial loads, are

evaluated.

Results of the energy analysis are used to perform the economic analysis based on some financial parameters such as the net present value, the pay-back period and the profitability index. By taking into account the electricity, heat and hydrogen markets in different pricing scenarios, different plant management options are investigated and analyzed.

Thus, the relevance of this paper is due both to the study of the co-production of more energy services by using the same plant, whose behavior and performances are relatively unexplored, and to the evaluation of the flexibility and profitability of this system with referring to the current, short and target technological development scenarios under current and future energy vectors markets.

2. Energy and Economic analysis procedure

This study has been carried out in 3 main steps. At the beginning, the plant lay-out has been defined according to the project idea to produce hydrogen, heat and electricity by using biogas (available from anaerobic digestion process) as primary source and an SOFC power unit as prime mover.

As second step, the energy assessment has been performed by using a simulation tool that has allowed to implement the plant-lay-out and to assign the operating conditions to streams and components.

Finally, results of the energy analysis have been used to perform the economic assessment of the proposed plant in different management strategies. In figure 2 the blocks diagram of the procedure followed for energy and economic analysis is illustrated.

For reaching the aim of the study it has been very important to create and define a flexible plant design and management that permits to evaluate the optimal conditions from energy and economic points of view.

As reported by Ma et al. [19], the flexibility can be classified in flexibility "on" engineering systems and flexibility "in" engineering systems. Typically, flexibility options "on" engineering systems are recognized as operational flexibility where managerial decision rules are based on the system operation and management. Flexibility options "in" engineering systems are referred to a constructional flexibility, which focuses on the modularity embedded in the process system design. In this study the analysis approach refers to the flexibility "on" engineering systems and is carried out by defining four management strategies to balance the electricity generation and the complementary hydrogen production, basing on the variable electrical price while the thermal output is maintained constant.

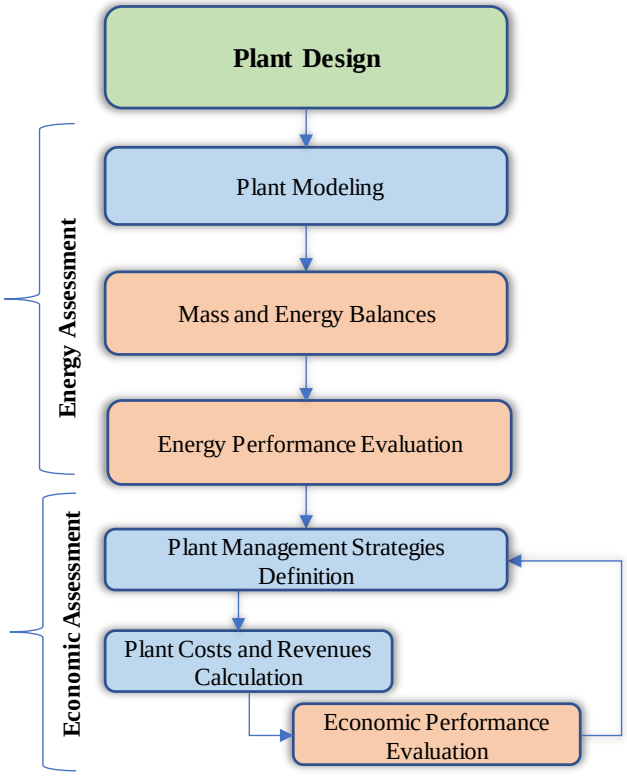

Figure 2. Block diagram of the energy and economic analysis

3. Plant design

The plant design regards the polygeneration system of the MES as depicted in figure 1. This means that the Anaerobic Digester (AD) section, and consequently the bio-chemical conversion of the biomass into biogas, has not been considered. The biogas composition has been assumed

equal to 60% CH_4 and 40% CO_2; this is the composition expected by using the BEKON Dry Fermentation technology [20], that has been chosen as the Best Available Technology for the anaerobic digestion process. Figure 3 shows the lay-out of the polygeneration system.

Biogas, air and water are heated in the heat exchangers HE2 (300°C), HE3 (580°C) and HE4 (580°C), respectively, before entering the ATR reactor (Autothermal Reforming Reactor).

The autothermal reforming (ATR) combines the partial oxidation reforming and the steam reforming in a single process in which the thermal energy, needed to sustain the endothermic reforming reaction, is internally supplied by the oxidation of a portion of processed fuel with a controlled amount of oxidant. Thus, the operating parameters of the process are the pressure, the temperature (or the oxidant to carbon ratio, here defined as the air to biogas ratio, A/B) and the steam to carbon ratio (here defined as the steam to biogas ratio, S/B) [21].

High reforming temperatures assure higher hydrocarbon conversion as suggested in [22-24].

The produced syngas exiting the ATR, is cooled at 320°C (HE7) and then is separated in two fluxes: the stream (7) is sent to the WGSR (water gas shift reactor) and the stream (AN-IN) is used for feeding the SOFC power unit. The air for the SOFC cathode side (1) of the SOFC is pre-heated before entering in the cathode (CATH-IN) at about 400 °C.

The stream exiting the WGSR is cooled in the heat exchanger HE8 and dried in the SEP before to be compressed (compressor C) to 8 bars and heated (HE5) to reach the operating conditions of the membrane separation unit (Pd-M), where the product hydrogen is recovered.

Currently, various gas separation technologies are readily available for separating hydrogen from the synthesis gas by reforming or gasification processes; the membrane separation technology has shown several advantages such as low energy consumption, environmentally friendly characteristics and the promising potential of using as a multifunctional membrane reactor [25]. In comparison with other hydrogen separation technologies, like pressure swing adsorption (PSA), membrane gas separation offers simplicity of operation, less energy demand,

small footprint, continuous operation, easy scale-up, etc. For this reason, in this study the hydrogen separation based on the membrane technology has been selected.

Thus, the pure hydrogen (12) is cooled (HE9) and compressed (IC) at 820 bars, in accordance to the requirements of a hydrogen refilling station, while the purge gas (13) is combusted in a catalytic burner (CB) together with the cathode off-gas (CATH-OFF), the anode off-gas (AN-OFF) and the fresh air (2). The combustor effluent exchanges heat with more streams (heat exchangers HE3, HE4, HE5, HE6), before being exhausted (22) at 105 °C. The heat exchangers devoted to the thermal demand are HE6, HE7, HE8 and HE9.

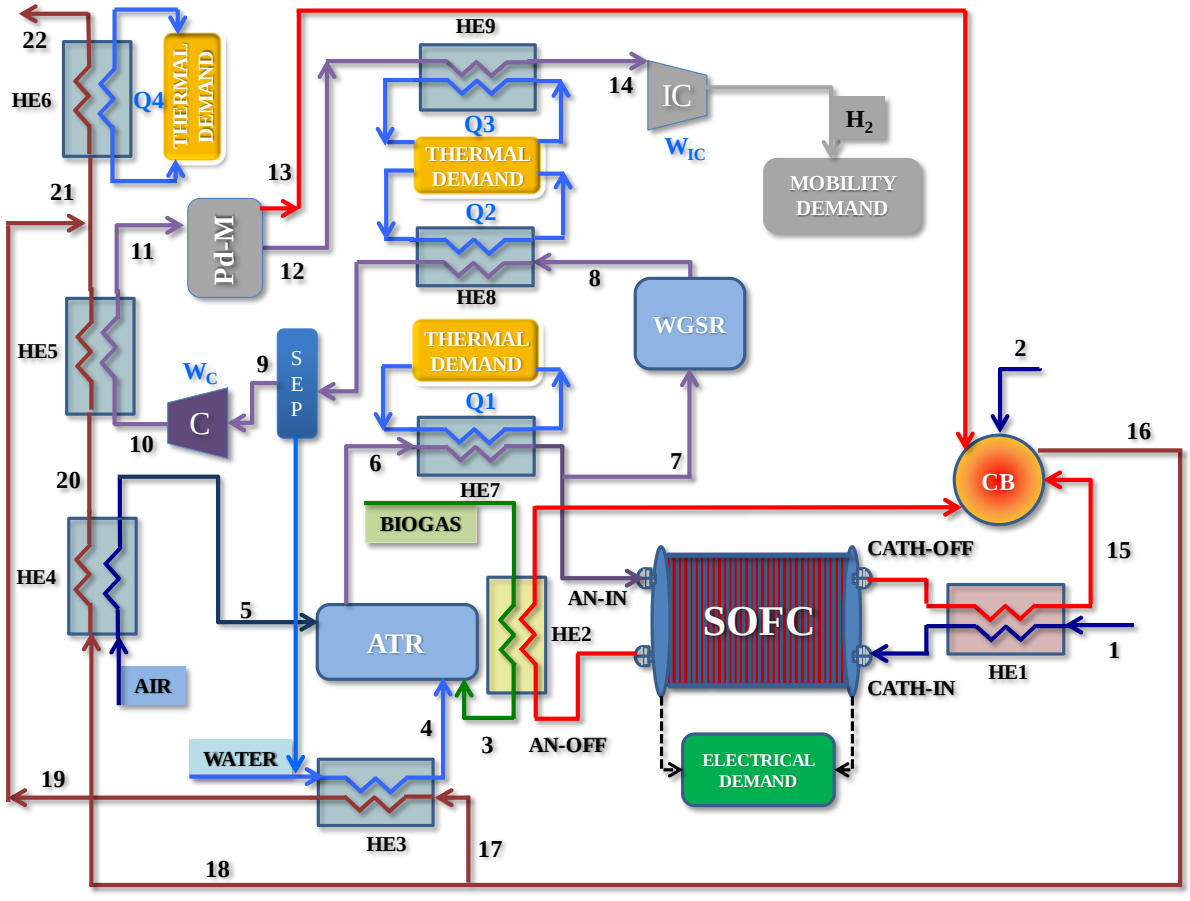

Figure 3. Lay-out of the polygeneration system

4. Energy Assessment

4.1 Plant Modeling

The objective of the polygeneration plant modeling is to provide the system characterization in terms of mass and energy balances as well as to forecast its performances in order to support the decision making at the design, operating and control levels. Therefore, the modeling of the plant units requires the knowledge of the fundamental phenomena, i.e. thermodynamic, transport (mass transfer and heat transfer) and chemical processes that can occur in each component.

The energy model of the polygeneration plant has been built by using the Aspen Plus software package, a commercial flowsheet simulator widely used from industry and academic researchers for complex energy systems simulation [26]. Aspen Plus is a computer-aided software which uses mathematical algorithms based on thermodynamic models, physical relationships and properties methods, to define the system characteristics (stream properties, operating conditions of plant components, equipment sizes, etc.) and to predict the system performance. Moreover, sensitivity analyses can be carried out on thermodynamic and chemical parameters in order to investigate their influence on system performance and to optimize the plant operating conditions.

Therefore, in the plant model, each sub-system is simulated by means of operation blocks and/or calculator blocks, interconnected through mass, energy, or information flows.

Figure 4 shows the flowsheet of the model that integrates the sub-models of each system unit by means of five Hierarchy blocks whose inlet and outlet streams are labeled according to those defined in figure 3. Thus, each hierarchy block represents a specific section of the plant, for example the biogas processing unit (BPUNIT) or the SOFC power unit (SOFC), modeled in a sub-flowsheet by combining operation blocks and calculator blocks for components and processes simulation.

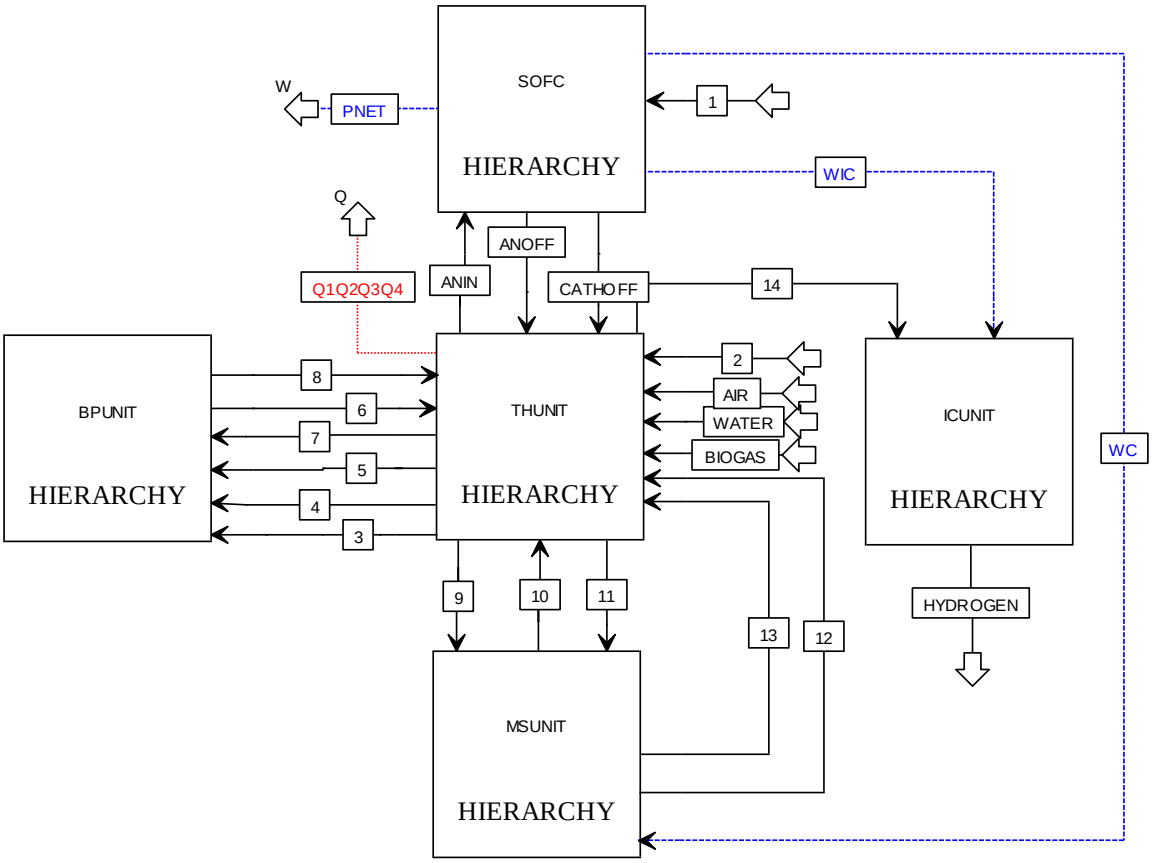

Figure 4. Flowsheet of the polygeneration system model

They are:

-BPUNIT (Biogas Processing Unit): it consists of an autothermal reactor and a water gas shift reactor.

-SOFC (SOFC Power Unit): the power unit consists of SOFC modules each of which is formed by stacks. Thanks to the modular configuration each stack is modeled by means of a single-cell model up-scaled to stack level.

-MSUNIT (Membrane Separation Unit): it consists of a compressor to reach the membrane operating pressure and the membrane separation modules.

-ICUNIT (Ionic Compressor Unit): it consists of a multistage compressor.

-THUNIT (Thermal Unit): in this hierarchy block the thermal balance of the plant, according with the thermal fluxes and heat exchanges shown in figure 3, is modeled. Therefore, it consists of eight heat exchangers, a dryer for water separation (stream 8) and a catalytic burner.

There are several parameters that can be assigned in the simulation model. For the reactors, must be specified pressure and temperature or heat duty. The temperature of each reactor can be set to different values according with the reactor's purpose (reforming, water gas shift). The Peng-Robinson physical property method, particularly suitable for hydrocarbons and light gases, such as carbon dioxide and hydrogen, has been chosen and applied for the calculations of all streams.

A description of the sub-models is presented in the following. Some of which have been developed and presented by the authors in previous papers, so that details on governing equations, physical, fitting and calibration parameters as well as on the validation procedure are omitted.

4.1.1 Biogas Processing Unit

In order to maximize the hydrogen production, the reforming process in the biogas processing unit is carried out in two steps: i) high-temperature step (the main reactions are the partial oxidation and the steam reforming), in which the fuel is converted into a gaseous mixture of H_2, CO, CO_2, N_2, and H_2O; ii) low temperature step (the main reaction is the water gas shift), in which CO is reacted with H_2O towards H_2 and CO_2. As a result, the biogas processing unit consists of an ATR reactor and a WGSR reactor. Due to the operating temperature of the shifter (about 200-400°C), the syngas coming from the ATR must be cooled before entering the WGSR.

The autothermal reforming process is investigated by assuming that the residence time inside both in the ATR and WGSR the reactors is enough, so that all chemical reactions reach

equilibrium stage. The chemical equilibrium is solved by applying the direct minimization of the Gibbs free energy for a given set of species. This non-stoichiometric method allows to find the equilibrium composition when the reactions system is unknow or very complex. Thus, the hypothesis is that by reaching the chemical equilibrium the gas system can be formed by H_2, CO, CO_2, H_2O, N_2, CH_4, C(s). For the autothermal reforming reactor, working at atmospheric pressure, the equilibrium composition has been calculated by fixing the operating temperature and the S/B ratio, whereas, for the water gas shift reactor only the operating temperature is assumed as data input (for the chemical equilibrium calculation, the CH_4 in the inlet stream is considered as an inert). In table 1 the blocks used in the BPUNIT hierarchy flowsheet are summarized.

Table 1. Blocks used in the BPUNIT hierarchy

Hierarchy Component	Block Type	Inputs	Outputs
Autothermal Reformer (ATR)	Unit Operation RGibbs: RGibbs models chemical equilibrium by the minimization of Gibbs free energy	Pressure, temperature, S/B, product species	A/B, syngas compositions and properties
Shifter (WGSR)		Pressure, temperature, product species	Syngas compositions and properties

4.1.2 SOFC power unit

The simulation of the SOFC power unit is performed by means of a single cell numerical model developed in previous works [27,28], that allows to forecast the cell performance under different working parameters such as pressure, temperature, inlet gas compositions, anode and cathode utilization factors and flow configurations. The cell physical domain (anode, cathode and electrolyte) is discretized in N-elements throughout the flow direction and mass and energy balances are sequentially solved, for each element, by considering the electrochemical and thermochemical reactions occurring in the anode and cathode sides.

In the single-cell modeling, the anode is simulated by a stoichiometric reactor block RStoic in which the electro-oxidation reaction takes place and a RGibbs reactor block in which the reforming reaction and/or the water gas shift reaction that can occur during the fuel cell

operation are considered. The cathode side is modeled by a Sep block in which the oxygen is separated from the incoming cathode flow and sent to the anode side according to the assigned utilization factor. Moreover, a heat exchanger to simulate the preheating of the cathode air is also considered.

In order to extend the single cell model to the stack level, a performance parameter widely used to quantify the overpotential losses linked to the fuel cell operations, the cell area-specific resistance (ASR, Ω cm^2), has been employed. The ASR_{cell} is defined as:

$$ASR_{cell} = \frac{OCV - V_{cell}}{j_{cell}} \quad (1)$$

where OCV is the open circuit voltage (V), V_{cell} and j_{cell} are the cell voltage (V) and the current density (Acm^{-2}), respectively. Therefore, because the up-scaling from small single cell to stack level involves a drop-in performance due to the complexity for achieving a homogeneity in electrical contact and gas distribution, a stack loss factor has been introduced [28]:

$$f_{stack} = \frac{ASR_{stack}}{ASR_{cell}} \quad (2)$$

Thus, the stack voltage can be calculated as:

$$V_{stack} = ASR_{stack} j_{cell} n_{cell} \quad (3)$$

where n_{cell} is the cells number in the stack.

The energy balance of the SOFC is solved by using a Fortran block calculator (SOFC energy balance, SOFCEB) where the cell electrochemical model is implemented, a mixer block (SOFC thermal fluxes, SOFCTF) and a splitter block (SOFC energy fluxes, SOFCEF). The mixer block sums the thermal fluxes due to: i) the sensible enthalpy changes of the feeding stream at the anode and cathode, ii) the electrochemical reactions occurring at the anode and cathode side and iii) the chemical reactions (steam reforming and water gas shift) occurring in the anode

side. The splitter block is used to separate the total energy flux in the electrical power and the net thermal power generated during the SOFC operation and calculated by means of the Fortran calculator block. Table 2 lists the blocks used for the SOFC modeling and their main features.

Table 2. Blocks used in the SOFC Hierarchy

Hierarchy Component	Block type	Inputs	Outputs
Anode	Unit Operation RStoic RStoic models a reactor when stoichiometry is known	Pressure, temperature, Stoichiometric reaction H2/O2, extent of reaction	Stream composition and properties, flow rate, energy balance
	Unit Operation RGibbs. RGibbs models chemical equilibrium by the minimization of Gibbs free energy	Pressure, temperature	Stream composition and properties, flow rate, energy balance
Cathode	Unit Operation Sep. Sep combines inlet streams and separates the resulting stream into two or more streams, according to the specification for each component.	Pressure, temperature, oxygen split fraction	Streams composition, flow rates, energy balance
Heat Exchanger	Unit Operation HeatX. HeatX can perform shortcut or detailed rating calculations for most types of two-stream heat exchangers.	Pressure, temperature of cold stream	Streams properties, Heat duty
SOFC Thermal Fluxes (SOFCTF)	Unit Operation Mixer. Mixer combines material streams (or heat streams or work streams) into one outlet stream	Heat streams from the unit operation blocks of the SOFC hierarchy flowsheet	Total heat stream
SOFC Energy Fluxes (SOFCEF)	Unit Operation FSplit. FSplit separates an input stream (material or energy, heat/work) into two or more outlet streams of the same type (material or energy, heat/work)	Total heat stream from SOFCTF. Calculated data from SOFCEB	Heat and work streams
SOFC energy balance (SOFCEB)	Fortran Calculator. User defined electrochemical model [27,28]	Pressure, temperature, streams compositions, electro-chemical parameters, cell area, etc.	Stack polarization curve, stack electric power, stack thermal power, stream compositions, flow rates, etc

4.1.3 Membrane separation unit

Among the membranes available for hydrogen separation, dense metal membranes based on Pd-alloys (Pd-Ag, Pd-Cu, Pd-Au, Pd-Ag-Au) have recently received considerable attention thanks to their excellent hydrogen permeability, high tolerance to hydrocarbon flows, high

resistance to H2S poisoning, excellent resistance to hydrogen embrittlement and catalytic ability for hydrogen recombination [29].

They can be classified in two main groups, unsupported (i.e. self-supporting membranes), usually prepared from relatively thick palladium foils and supported ones (i.e. composite Pd-based membranes) in which a selective thin layer is incorporated on the surface of a porous material, composed of ceramic or stainless steel, that provides the required mechanical resistance [29,30]. In comparison with unsupported membranes, the hydrogen permeance is higher so that less membrane area is required and the whole membrane cost will be lower [31]. Therefore, it is foreseen that dense composite membranes have the best chance to be first commercialized for large-scale pure hydrogen production. Currently, there are some companies and research institutes providing dense metal membrane products and system solutions for hydrogen separation and many pilot-scale demonstration studies are being conducted [28,31].

Thus, in this study, the membrane separation unit is based on supported ceramic Pd-Ag membrane and it is formed by multi-tube membrane modules, similar to the pre-commercial Hysep modules manufactured by the ECN Research Centre [31].

The membrane sub-model, developed in previous works [9,32], is briefly described in the following. The hydrogen permeation process through a metallic film involves the dissociation of hydrogen molecule into hydrogen atoms on the high-pressure side (feed side) of the film, then the diffusion through the film and the re-association on the low-pressure side (permeate side).

The hydrogen permeation flux through the membrane is described by the following relationship:

$$J_{H_2,perm} = \frac{Pe}{s} \cdot \Delta P \tag{4}$$

where Pe ($m^3\ m^{-1}\ s^{-1}\ Pa^{-0.5}$) is the hydrogen permeability, s (m) is the membrane tube thickness and ΔP ($Pa^{0.5}$) is the driving force of permeation calculated as defined in [9].

The hydrogen recovery factor (*HRF*), calculated as the ratio between the flow rate of the H_2 permeated through the membrane and the H_2 feed flow rate, is the parameter used to evaluate the efficiency of the permeation process:

$$HRF = \frac{n_{H_2,perm}}{n_{H_2,feed}} \quad (5)$$

The hydrogen permeation flow rate (mol s^{-1}) is given by:

$$n_{H_2,perm} = J_{H_2,perm} \cdot A_{perm} \quad (6)$$

where A_{perm} (m^2) is the permeation area that is obtained by combining Eqs. 4,5,6.

Because of the multi-tubes configuration of the membrane module, the total membrane permeation area A_{perm} is also equal to:

$$A_{perm} = N_m N_t \cdot A_{perm,tube} \quad (7)$$

where $A_{perm,tube}$ is the single tube permeation area, N_m the modules number and N_t the number of tubes in each module.

The sizing of the membrane separation unit, performed through an iterative procedure that allows to minimize the total permeation area, is carried out by assigning the membrane thickness, the hydrogen recovery ratio *HRF*, the feed and the permeate sides pressures and the membrane operating temperature.

The model of the membrane separation unit has been implemented in Fortran language in the MS (Membrane Separation) sub-model. Table 3 summarizes the blocks used in the MSUNIT hierarchy flowsheet.

Table 3. Blocks used in the MSUNIT hierarchy

Hierarchy Component	Block type	Inputs	Outputs
Syngas Compressor (C)	Unit Operation Compr. Compr calculates either the power requirement given an outlet pressure specification, or the outlet pressure given a power specification.	Polytropic efficiency, pressure ratio	Stream properties, net power required
Membrane	Fortran Calculator.	Feed pressure, permeate pressure, stream composition,	Streams composition and

	User defined membrane model	hydrogen permeance, membrane thickness, tube diameter, HRF, etc	flow rates, number of tubes, number modules, membrane area

4.1.4 High pressure hydrogen storage

In refueling stations, the high-pressure storage of hydrogen in tanks requires the compression of hydrogen to more than 700 bars. Most compressors used today are either positive displacement compressors or centrifugal compressors. Positive displacement compressors can be reciprocating or rotary. In the field of reciprocating engines, a novel compressor configuration, in which the solid piston is replaced by a liquid piston, has been introduced in 2002 by Linde [33, 34]. The liquid piston compression, realized with ionic liquid compressor, has been proposed as a concept to improve the behavior and efficiency of the gas compression. Ionic liquids are room temperature salts with very low vapor pressures that can act the same as a solid piston for compressing hydrogen inside the compression chamber.

In this study this technology has been chosen for compressing hydrogen until to 820 bars [35] that is the high-pressure hydrogen storage in novel refueling stations.

Thus, the model of the ionic compressor (like to the ionic compressor IC-90 manufactured by Linde Group), developed in a previous paper [9], has been applied for simulating the compression and storage section of the polygeneration system. As illustrated in ref. [9], the ionic compressor has been modeled as an intercooled compressor consisting of 5 stages (pressure ratio of 2.8 for each stage) that work in near-isothermal conditions. Each stage consists of a polytropic compressor and a heat exchanger in which the removed thermal power is a percentage (90%) of the power required by the corresponding compressor [36]. In table 4 the blocks used in the ICUNIT hierarchy are listed.

Table 4. Blocks used in the ICUNIT hierarchy

Hierarchy Component	Block type	Inputs	Outputs
Hydrogen compression stage	Unit Operation Compr. Compr calculates either the power requirement given an outlet pressure specification, or the outlet pressure given a power specification.	Polytropic efficiency, pressure ratio	Stream properties, net power required
	Unit Operation Heater Heater produces one outlet stream.	Heat duty (cooling power)	Stream properties

4.1.5 Thermal Unit

The thermal management of the system is performed by using several heat exchangers that are used both to heat/cool the streams according to the required/assigned temperatures and to produce heat for the utility. The heat exchangers HE6, HE7, HE8 and HE9 are devoted to produce hot water for thermal demands; for these components the thermal efficiency has been assumed equal to 0.85. The thermal efficiency of the gas/gas heat exchangers (HE1, HE2, HE4, HE5) has been assumed equal to 0.75.

In order to account for the off-design conditions, the thermal efficiencies of all the heat exchangers vary from their maximum values (0.85 or 0.75) to a minimum value (about 0.65). Furthermore, the syngas drying (component SEP in figure 3) is simulated by means of a separator block, whereas the catalytic burner in which the SOFC off-gases are burnt is modeled as an RStoic block, by assuming adiabatic conditions and the flue gas temperature of about 880°C. Table 5 reports the blocks employed in the THUNIT hierarchy flowsheet.

Table 5. Blocks used in the THUNIT hierarchy

Hierarchy Component	Block Type	Inputs	Outputs
Water separator (SEP)	Unit Operation Sep. Sep combines inlet streams and separates the resulting stream into two or more streams, according to the specification for each component.	Stream composition and properties, fractional water separation	Streams properties and compositions

Catalytic Burner (CB)	Unit Operation RStoic. RStoic models a reactor when stoichiometry is known	Pressure, combustion reactions, adiabatic conditions, temperature	Stream properties, additional air flow rate
Heat Exchangers	Unit Operation HeatX. HeatX can perform shortcut or detailed rating calculations for most types of two-stream heat exchangers.	Pressure, heat removed/supplied	Streams properties

4.2 Mass and Energy balances

In order to define the SOFC power unit configuration in terms of modules number, stacks number and cells number per stack, the single cell polarization curve is calculated by considering the cell characteristics reported in [27]. Then, the cell-stack voltage has been estimated by applying Eqs. 2 and 3, in the operating voltage range OCV-V_{nom}. The current density and the fuel utilization factor equal to 0.5 A/cm^2 and 0.8, respectively, are chosen as stack operating parameters. Moreover, in order to simplify the stack thermal management, the stack cooling is performed by the anode and cathode flow rates (the air utilization factor is kept in accordance with the working conditions of the single SOFC described in [27], so that the optimal stack temperature is 800°C: the cell operating voltage results equal to 0.75 V. By fixing the cell area (500 cm^2), the SOFC power unit, sized for the maximum syngas flow rate coming from the BP unit, consists of 10 modules (each module is formed by 2 stacks with 55 cells per stack). This configuration allows to manage the power unit almost at the stack nominal power also at partial loads.

The design of the membrane separation unit, sized for the maximum hydrogen production, has been performed by fixing the hydrogen recovery factor *HRF* and by assuming, for the other designing data, values consistent with the structural, geometric and operating parameters of the pre-commercial module Hysep 1308 developed by the ECN Research Centre.

The ionic compressor has been modeled by assuming the operating data, in terms of polytropic efficiency and thermal power removed in each stage, that permit to simulate its near-isothermal conditions according to the specifications declared by Linde [36].

Table 6 lists the main input/output data of the polygeneration system. The modular architecture allows to maintain the same efficiency also when the hydrogen production or the SOFC load is reduced, according with the plant regulation strategies.

Table 6. Main input/output data of the polygeneration system

Plant Sections and Components	Input/Output data
Biogas Processing Unit (BPUNIT)	
ATR (Autothermal Reformer)	
Pressure (bar)	1.013
Temperature (°C)	771
Steam to Biogas ratio (S/B) (kg/kg)	0.8
Air to biogas ratio (kg/kg)	1.8
WGSR (Water gas shift reactor)	
Pressure (bar)	1.013
Temperature (°C)	400
SOFC Power Unit	
Power Modules	10
Stacks number	2
Cells number x stack	55
Active area (cm^2)	500
Stacks Temperature (°C)	800
Fuel utilization factor, U_F	0.79
Average cell voltage (V) at nominal power	0.75
Current density (A/cm^2) at nominal power	0.50
ASR_{stack} (Ωcm^2)	0.45
Stack electric power (kW)	10.2
Membrane Separation Unit (MSUNIT)	
Hydrogen Recovery Factor, HRF	0.74
Feed side pressure (bar)	8.0
Permeate side pressure (bar)	1.1
Operating Temperature (°C)	400
Hydrogen Permeability ($m^3\ m^{-1}\ s^{-1}\ Pa^{-0.5}$)	$1.39 \cdot 10^{-8}$
Modules Number	14
Module Tubes Number	18
Tube thickness (m)	$9.00 \cdot 10^{-6}$
Tube length (m)	1
Tube permeation area (m^2)	$3.85 \cdot 10^{-2}$
Hydrogen permeation flux x tube (mol $m^{-2}\ s^{-1}$)	$8.82 \cdot 10^{-2}$
Module permeation area (m^2)	0.69
Syngas Compressor	
Pressure ratio	8
Polytropic efficiency	0.75
Ionic Compressor Unit (ICUNIT)	
Stage Pressure ratio	2.77
Stage Polytropic efficiency	0.91
Stage Heat removed (%)	90
Outlet temperature Stage 1 (°C)	36
Outlet temperature Stage 2 (°C)	47

Outlet temperature Stage 3 (°C)	58
Outlet temperature Stage 4 (°C)	65
Outlet temperature Stage 5 (°C)	69
Thermal Unit (THUNIT)	
Thermal efficiency of water-gas/gas-gas heat exchangers	0.85/0.75

The system behavior has been investigated by varying the SOFC electric load from 100% to 30% (the minimum load that permits to sustain the electric power consumption of the hydrogen separation and compression units). Thus, four operating conditions, related to different SOFC loads, have been analyzed. Modeling results, in terms of temperature and mass flow rate of each streams (see figure 3) are illustrated in table 7.

Table 7. Streams characteristics at different SOFC loads

Notation	**A**		**B**		**C**		**D**	
SOFC load	**30%**		**50%**		**80%**		**100%**	
Streams	Mass flows (kg/h)	Temp. (°C)	Mass flows (kg/h)	Temp. (°C)	Mass flows (kg/h)	Temp. (°C)	Mass flows (kg/h)	Temp. (°C)
BIOGAS	104.5	20	104.5	20	104.5	20	104.5	20
AIR	189.2	20	189.2	20	189.2	20	189.2	20
WATER	83.6	20	83.6	20	83.6	20	83.6	20
AN-IN	113.2	320	188.7	320	301.9	320	377.4	320
CATH-IN	185.4	400	308.9	400	494.3	400	617.9	400
AN-OFF	137.5	800	229.1	800	366.5	800	458.1	800
CATH-OFF	160.9	800	268.1	800	429.1	800	536.3	800
H2	6.2	69	4.4	69	1.8	69	-	-
1	185.4	20	308.9	20	494.3	20	617.9	20
2	144.2	20	144.2	20	144.2	20	144.2	20
3	104.5	300	104.5	300	104.5	300	104.5	300
4	83.6	580	83.6	580	83.6	580	83.6	580
5	189.2	580	189.2	580	189.2	580	189.2	580
6	377.4	771	377.4	771	377.4	771	377.4	771
7	264.2	320	188.7	320	75.5	320	-	-
8	264.2	399	188.7	399	75.5	399	-	-
9	229.7	20	164.2	20	65.7	20	-	-
10	229.8	158	164.2	158	65.7	158	-	-
11	229.8	400	164.2	400	65.7	400	-	-
12	6.2	400	4.4	400	1.8	400	-	-
13	223.6	400	159.7	400	63.9	400	-	-
14	6.2	20	4.4	20	1.8	20	-	-
15	160.9	257	268.1	257	429.1	257	536.3	254
16	666.2	883	801.2	808	1003.7	734	1138.7	697
17	399.7	883	480.7	808	602.2	734	683.2	697

18	266.5	883	320.5	808	401.5	734	455.5	697
19	399.7	126	480.7	183	602.2	238	683.2	262
20	266.5	453	320.5	451	401.5	448	455.5	446
21	666.2	118	801.2	210	1003.7	298	1138.7	336
22	666.2	105	801.2	105	1003.7	105	1138.7	105

As reported in table 7, SOFC load 100% means that the biogas is totally used for SOFC feeding, so that the section of the system regarding the compressed hydrogen production does not work. On the contrary, at SOFC load 30%, the system produces the maximum hydrogen flow rate (150 kg/day) and the minimum electric power. In table 8 the chemical composition of the main streams is summarized.

Table 8. Main streams composition

Stream	6	8	9	13
Chemical composition (mol%)				
H_2	25.7	32.7	38.4	13.9
CO	9.7	2.7	3.2	4.4
CO_2	11.4	18.3	21.5	30.1
H_2O	24.9	18.0	3.6	5.0
N_2	28.4	28.4	33.3	46.6

4.3 Energy performance evaluation

The system efficiencies have been calculated as follows.

The electrical efficiency is:

$$\eta_{el} = \frac{W}{\Phi_{Biogas}} \tag{8}$$

The thermal efficiency is:

$$\eta_{th} = \frac{Q}{\Phi_{Biogas}} \tag{9}$$

The hydrogen production efficiency, referred to the lower heating value (LHV) is:

$$\eta_{H2} = \frac{\Phi_{H2}}{\Phi_{Biogas}} \tag{10}$$

Thus, the overall efficiency in the co-production of fuel and power (electric and thermal) is [9]:

$$\eta_{CFP} = \frac{W + Q + \Phi_{H2}}{\Phi_{Biogas}} \quad (11)$$

In Eqs. (8) – (11), W is the net electric power, Q is the available thermal power, Φ_{H2} is chemical power of the product hydrogen (LHV is 120 MJ/kg) and Φ_{Biogas} is the chemical power of the biogas feeding the polygeneration system (LHV is 17.7 MJ/kg).

Furthermore, in order to evaluate the energy saving obtained by the polygeneration of electricity, heat and hydrogen with respect to their separate production in reference technologies, the energy saving factor (ES) has been introduced as further performance parameter:

$$ES = 1 - \frac{1}{\frac{\eta_{el}}{\eta_{el,ref}} + \frac{\eta_{th}}{\eta_{th,ref}} + \frac{\eta_{H2}}{\eta_{H2,ref}}} \quad (12)$$

where the electric, thermal and hydrogen reference efficiencies result to be equal to 42%, 75% and 64%, respectively. The reference electric and thermal efficiencies are the values suggested in [37] and referred to biogas-based plants, whereas the reference hydrogen efficiency is calculated by taking into account the energy consumption of alkaline electrolyzer technology (4.4 kWh/Nm^3_{H2} [38]) and the energy consumption for hydrogen compression and storage (2.7 kWh/kg_{H2} by applying the ionic compressor technology [34]).

Table 9 summarizes the thermodynamic performance of the polygeneration system. The net electric power ranges from 14.6 kW, corresponding to the SOFC load of 30% that is the minimum value able to satisfy the electric power consumption of the hydrogen separation and compression units, to 204 kW. By analyzing the thermal power production, it can be noted that the highest value (154.3 kW) is reached at the SOFC full load operation. This thermal power is totally due to the exhausts from the catalytic burner (Q4 at HE6) and from the heat exchanger HE7 (Q1) that is used to cool the syngas exiting the ATR from 771°C to 320°C. This last thermal power does not change by varying the SOFC load because the heat is recovered by cooling the total syngas mass flow rate (before to be split in two streams).

In table 9 the energy saving factor (ES) is also reported. It can be noted that the polygeneration system permits to achieve an energy saving in the whole operating range. The energy saving rises with the increasing of the electric load and reaches 25.7% as the SOFC works at rated power (100% load).

Table 9. Perfomances in the operational range (Φ_{Biogas} = 513.5 kW)

Notation		A	B	C	D
SOFC load		30%	50%	80%	100%
Thermal Power (kW)	Q_1	68.4	68.4	68.4	68.4
	Q_2	69.5	44.7	13.9	-
	Q_3	9.5	6.1	1.9	-
	Q_4	1.8	19.8	56.3	85.9
	Q	149.2	139.1	140.5	154.3
Electric Power (kW)	W_C	24.9	14.2	5.7	-
	W_{IC}	22.5	16.1	6.4	-
	W_{SOFC}	62	102	164	204
	W	14.6	71.7	151.9	204
Chemical Power (kW_{LHV})	Φ_{H2}	207.3	148.0	59.3	-
Electrical efficiency (%)	η_{el}	2.8	14.0	29.6	39.7
Thermal efficiency (%)	η_{th}	29.1	27.1	27.4	30.1
Hydrogen production efficiency (%)	η_{H2}	40.4	28.8	11,6	0.0
Overall efficiency (%)	η_{CFP}	72.3	69.9	68.5	69.8
Energy saving factor (%)	ES	7.9	12.6	20.0	25.7

It is worth nothing that the overall efficiency (CFP efficiency) trend is almost constant as the electric load varies. The minimum value is 68.5 % (at 80% SOFC load) while the maximum efficiency of 72.3% is reached at the minimum SOFC load (30%); this result shows that, from the overall performance point of view, the best value is obtained when in the system the highest hydrogen rate is produced. On the other hand, as it is expected, the electric efficiencies and the hydrogen production efficiencies increase and decrease, respectively, with the SOFC load. The thermal efficiency ranges from 27.1% (50% SOFC load) to 30.1% at the maximum SOFC load.

5. Economic Assessment

After the energy analysis, the evaluation of the total capital investment and the assessment of the economic revenue and the main economic indicators, such as Profitability index, Net Present Value (NPV), Internal Rate of Return (IRR) and Discounted Payback Period (DPBP), have been performed and MES the economic feasibility has been defined.

This analysis has been conducted by considering the whole MES and not only the polygeneration section, because the operating and maintenance (O&M) costs of the AD section are included in the analysis (the AD investment cost is not considered because a refit option has been assumed).

The economic assessment has been developed to identify the most promising management strategy, basing on main economic indicators under different technological developments and market scenarios, by assuming the polygeneration system lifetime equal to 20 years.

5.1 Plant Management Strategies Definition

By considering the electrical price variable in the time, four management strategies (able to balance the electricity generation and the complementary hydrogen production), have been defined.

According to the Directive 2012/27/EU of the European Parliament and of the Council of 25 October 2012 on energy efficiency, the electrical production is supposed to be dispatched to the grid by operating the polygeneration system within an aggregate of little generators that act as Virtual Power Plant (VPP) [39], a production option that is indicated as one of the solutions to increase the grid resilience [40]. Under this hypothesis, the market electrical price mirrors the value of this commodity under a grid stability perspective: i) during the peak period, characterized by high electrical demand, the price of the electricity is high; ii) during the off-peak period, characterized by low electrical demand, the electricity price is low.

Moreover, in a grid stability perspective, the Ancillary Services can be also considered as a management strategy option. In most electricity markets, offering frequency regulation to the grid operator means that the generator is willing to increase the power (called "regulation up") or decrease the power ("regulation down") by some amount. This means that the generator is removing capacity from the day-ahead/real-time energy market (AS down condition) and is committing to being able to produce some amount of power (AS up condition). Thus, in this case, in order to balance the grid requirements, the VPP can be available to change on line its production rate, obtaining an economical reward.

Therefore, four management strategies, described in table 10, are proposed. Moreover, for the mobility management strategy, an additional plant configuration (Mobility SU), obtained by downsizing the SOFC power unit, is also considered for the economic analysis.

Table 10. Management Strategies

Management Strategy	**Description**
Base Load	The MES produces always the maximum electrical load (hydrogen is not produced). The SOFC is sized to supply a nominal power of 204 kW.
Peaker	The MES regulates the electrical production within the peak and off-peak periods; in order to maximize the earning, it operates at maximum load during the peak period (higher price for electricity) and at minimum load during the off-peak period (lower price for electricity) switching to the hydrogen production. The SOFC is sized to supply a nominal power of 204 kW.
Ancillary Service	The MES takes part to the Ancillary Market in the so-called Secondary Frequency Control, which aims to restore the grid frequency to its nominal value by varying the load provided by the power unit in the range of few minutes [41]. During the off–peak period, in case of low grid frequency, the MES offers to increase its load from 30% up to 50% (AS up condition); on the contrary, during the peak period, in case of high grid frequency, the load of the MES is reduced from 100% to 80% (AS down condition). These actions are triggered by the Transmission System Operator and rewarded accordingly. The SOFC is sized to supply a nominal power of 204 kW.
Mobility	The MES is operated to maximize the hydrogen production. Thus, the SOFC works at 30% of the rated power. The SOFC is sized to supply a nominal power of 204 kW.
Mobility SU (Small Unit)	This additional strategy is also considered in the economic analysis, because the Mobility strategy could be also implemented downsizing the power unit. In this case, the

components of the hydrogen production section are sized for generating the maximum hydrogen flow rate, whereas the SOFC power unit is sized to self-sustain the system electric demand (The SOFC size is 64 kW).

For all the management strategies, a full-year of operation, equal to 8000 h (in accordance with the yearly Anaerobic Digester availability and as a consequence with the biogas availability), is assumed. Start and stop events are reduced to the minimum, thanks to the hydrogen production operation mode during the low electricity price period, a condition which is beneficial for the SOFC stacks life.

Table 11 lists the hourly distribution between the different SOFC loads for each management strategy.

Table 11. Hourly distribution between the different SOFC loads for each management strategy

		SOFC load (%)			
		SOFC 30% A	SOFC 50% B	SOFC 80% C	SOFC 100% D
Management Strategy	MES Energy Vectors	Operational time distribution* (h)			
		h_A	h_B	h_C	h_D
Base Load	Electricity/Heat	0	0	0	8000
Peaker	Electricity/Heat/Hydrogen	4800	0	0	3200
Ancillary Service	Electricity/Heat/Hydrogen	3692	1231	615	2462
Mobility	Hydrogen/Heat	8000	0	0	0

**Annual operational time is 8000 h*

In the Base Load strategy, the system operates always at the maximum SOFC load (100%), while, in the Peaker strategy, the operational time is split between the 30% SOFC load (during the off-peak period) and the 100% SOFC load (during the peak period).

In the Ancillary strategy, the MES is operated in all considered SOFC loads: i) at the maximum SOFC load for the 31% of the total operational time (during the peak period); ii) at the minimum SOFC load for the 46% of the total operational time (during the off-peak period); iii) at the 50% and 80% of the nominal SOFC load for the remaining operational time (the AS up condition occurs with a double frequency than the AS down condition). These hypotheses are based on the historical Ancillary Service data in the Italian Market [42]

In the Mobility strategy the SOFC operates always at minimum load to assure the maximum hydrogen production.

Table 12 reports the yearly system energy production taking into account the system operation according to each management strategy. It is worth nothing that the Base Load (8000 hours) and Mobility (8000 hours) management strategies mirror the specific results obtained by operating the SOFC power unit at 100% and 30% of the rated power (see table 9), with a higher efficiency for the hydrogen production, and a higher energy saving for the Base Load strategy.

Table 12. Energy Performances of the polygeneration system vs management strategy

	Base Load	**Peaker**	**Ancillary Service**	**Mobility**
Electricity (MWh/year)	1632.0	722.9	737.8	116.8
H_2 Chemical Energy (MWh/year)	-	995.0	984.1	1658.4
Heat (MWh/year)	1234.4	1209.9	1188.2	1193.6
Biogas Chemical Energy (MWh/year)	4108.0	4108.0	4108.0	4108.0
Average Overall Efficiency (%)	69.8	71.2	70.8	72.3
ES (%)	25.7	15.9	15.7	7.9

The Peaker and the Ancillary Service strategies introduce an intermediate condition, with the latter characterized by slightly lower efficiency and energy saving with respect to the Peaker one.

5.2 Plant costs and revenues calculation

The initial investment for capital expenditure (CAPEX) has been evaluated considering the specific cost of the equipment involved in the polygeneration layout. This means that the investment cost of the Anaerobic Digester is not considered (the polygeneration system has been integrated within an already existing AD as a refit option).

Moreover, the total cost of the polygeneration system has been projected over three different Technological Development Scenarios (TDS). They are: i) Current TDS based on 2018 costs, ii) Short-term TDS with a 2030 horizon and iii) Target TDS to be reached within 2050.

Several analyses on the SOFC cost and on its reduction expected in the mid and long terms have been made both by the US Government [43,44] and the European Community [45,46]. In this study the cost of the SOFC system is based on the European perspective that is less optimistic. Moreover, in the mid and long terms, a costs reduction both for the Pd-based membranes and the Ionic Compressor, is foreseen. With respect to the replacement costs, the substitution of the SOFC stack and the replacement of the catalysts of chemical reactors are fixed every 10 years and 6 years, respectively. Table 13 reports the evaluated CAPEX and replacement costs for the polygeneration system in the current, short-term and target scenario of technological development.

Table 13. CAPEX for the polygeneration system in the current, short-term and target scenario of technological development.

	CAPEX (k€)			Replacement Cost (k€)[a]		
	Current TDS	Short-term TDS	Target TDS	Current TDS	Short-term TDS	Target TDS
Ionic Compressor	1 875.0	1 500.0	1 200.0	-	-	-
204 kW SOFC [29]	1693.8	682.6	423.7	249.5[a]	110.2[a]	97.5[a]
ATR WGS Reactor	225	225	225	40.5[b]	40.5[b]	40.5[b]
Heat Exchangers	130	130	130	-	-	-
Pd Membrane	80	65	50	-	-	-
Measurement and Control	80	80	80	-	-	-
Piping & BOP	63	63	63	-	-	-
Civil Work	40	40	40	-	-	-

[a] *The mean time between replacement is 10 years [30]*
[b] *The mean time between replacement of catalysts is 6 years*

The operating and maintenance costs (O&M) have been estimated on a yearly basis at the 3% of the initial investment [45]. The Anaerobic Digester O&M costs are calculated by considering 15 k€/year for maintenance and 70 €/ton for the biomass (organic fraction of municipal solid waste). By assuming a volatile solids content of 70% and a methane production of 260 $Nm^3_{CH4}/tonn_{VS}$, the cost of the produced biogas is equal to 44.9 €/MWh for a production of 4110.3 MWh/year.

Table 14 summarizes the total costs for the three different technological development scenarios considered and for the two system configurations defined.

Table 14. Total costs for the MES (SOFC power unit 204 kW) and the MES-SU (SOFC power unit 62 kW) in the Current, Short-term and Target technological development scenarios

	MES 204 kW	MES-SU 62 kW
CAPEX (k€)		
Current TDS	4186.8	3007.8
Short-term TDS	2785.6	2310.5
Target TDS	2211.7	1916.8
Replacement Cost* (k€)		
Current TDS	371	197.3
Short-term TDS	231.7	155
Target TDS	219	151.1
O&M Cost (k€/year)		
Current TDS	125.6	90.2
Short-term TDS	83.6	69.3
Target TDS	66.4	57.5

**calculated over 20 years lifetime with zero discount rate*

The ability to dispatch different energy vectors is evaluated by defining the MES Annual Revenue (AR) for the defined management strategies; the following equations are used:

$$AR_{Base\ Load} = p_{E_W,peak} \cdot (W_D \cdot h_D) + p_{E_Q} \cdot (Q_D \cdot h_D) \quad (13)$$

$$AR_{Peaker} = p_{E_W,peak} \cdot (W_D \cdot h_D) + p_{E_W,off-peak} \cdot (W_A \cdot h_A) + p_{E_Q} \cdot (Q_D \cdot h_D) + p_{E_Q} \cdot (Q_A \cdot h_A) + p_{E_{H_2}} \cdot (\Phi_A \cdot h_A) \quad (14)$$

$$AR_{Ancillary\ Service} = p_{E_W,peak} \cdot (W_D \cdot h_D) + p_{E_W,off-peak} \cdot (W_A \cdot h_A) + p_{E_W,off-peak} \cdot (W_B \cdot h_B) + p_{E_W,ASup} \cdot [(W_B - W_A) \cdot h_B] + p_{E_W,peak} \cdot (W_C \cdot h_C) + \left[\left(p_{E_W,peak} - p_{E_W,ASdown}\right) \cdot (W_D - W_C) \cdot h_C\right] + p_{E_Q} \cdot (Q_A \cdot h_A + Q_B \cdot h_B + Q_C \cdot h_C + Q_D \cdot h_D) + p_{E_{H_2}} \cdot (\Phi_A \cdot h_A + \Phi_B \cdot h_B + \Phi_C \cdot h_C) \quad (15)$$

$$AR_{Mobility} = p_{E_W,off-peak} \cdot (W_A \cdot h_A) + p_{E_{H_2}} \cdot (\Phi_A \cdot h_A) + p_{E_Q} \cdot (Q_A \cdot h_A) \quad (16)$$

where $p_{EW,}\ p_{E_{H_2}}, p_{E_Q}$ are the prices of electricity, hydrogen and heat, reported in table 15. The prices of electricity refer to the peak/off-peak conditions, as derived by the Day-Ahead market

prevision; moreover, in the case of Ancillary Service the produced energy is paid as in the Day-Ahead, while the variation of production (from 30% to 50% according to the AS up condition and from 100% to 80% according to the AS down condition) is rewarded differently (see eq. 15). Two market scenarios, Present Market (PM) and Future Market (FM), have also been considered.

Table 15. Prices (€/kWh) of Energy Vectors in the Present and Future Markets

Energy Vector		Present Market	Future Market
Electricity	$p_{E_W,peak}$	0.080	0.080
	$p_{E_W,off-peak}$	0.060	0.040
	$p_{E_W,ASdown}$	0.025	0.010
	$p_{E_W,ASup}$	0.115	0.250
Hydrogen	$p_{E_{H_2}}$	0.330	0.240
Heat	p_{E_Q}	0.080	0.080

The electrical prices in the Present Market refer to the Italian market, as an average of the 2017 condition, provided by TERNA that is the Italian Transmission System Operator [42]. In the Future Market scenario, the electrical prices are defined considering the effects due to the expected increase of the share of electricity production from not programmable RES generators (wind and photovoltaic) which offer more energy at lower price but introduce also a higher grid unbalance risk. For the compressed hydrogen, the present price is 11 €/kg (0.330 €/kWh), aligned with the 2020 European target [47], while, for the Future Market, 8 €/kg (0.240 €/kWh), has been set, according to the targets for clean transportation defined in ref. [48]. The thermal energy production price is referred to the economic benchmark in terms of levelized cost of heating [46] for a condensing boiler and it is kept constant for both scenarios.

5.3 Economic Performance Evaluation

Table 16 shows the Net Annual Income comparison for the MES and the MES-SU.

As expected, the revenue from the full electricity production (Base Load management strategy), is not enough to cover the costs in all TDSs. This is mainly due to the low price of electricity both in the Present and Future Markets (the average electrical prices are 0.068 €/kWh and 0.056 €/kWh, respectively). The break-even average electrical price for the Base Load strategy should be 0.130 €/kWh in the Current TDS, 0.095 €/kWh for the Short-term TDS and 0.084 €/kWh for the Target TDS. These values could be reached with FIT incentives.

Table 16. MES and MES-SU net annual income (k€/year)

Energy vectors Market Scenario	Technology Development Scenario	Management Strategy				
		Base Load	Peaker	Ancillary Service	Mobility	Mobility SU
Present Market	Current TDS	-100.8	171.1	174.9	339.3	374.6
	Short-term TDS	-43.7	228.1	232.0	397.2	411.5
	Target TDS	-26.5	245.3	249.2	414.5	423.3
Future Market	Current TDS	-120.3	80.1	92.0	187.7	223.1
	Short-term TDS	-63.3	137.2	149.0	244.7	259.0
	Target TDS	-46.1	154.4	166.3	263.8	272.7

The Peaker and Ancillary Service management strategies, more devoted to the grid stability purpose, benefit from the hydrogen production. The Ancillary Service management strategy delivers more electrical energy and less hydrogen with respect to the Peaker, resulting anyway in a slight increase (about 1.8%) of the net annual income under Present Market and around 7.5% in the Future Market. This is due to the Ancillary Service revenues, which have higher specific impact.

The Mobility management strategy fully exploits the hydrogen price with a net annual income from 38% to 49.5% higher than the previous two strategies (Peaker and Ancillary Service). The better performance of the MES-SU is due to the reduction of the O&M costs.

A further economic comparison has been carried out by introducing the profitability index (not for the Base Load strategy that is economically negative):

$$Profitability\ Index = \frac{Present\ Value\ of\ future\ cash\ flow}{Initial\ Investment} \quad (17)$$

It is clear that a profitability index of 1.0 is the lowest acceptable value, whereas any value lower than 1.0 indicate that the project's present value (PV) is less than the initial investment. The PV is evaluated equal to 0.1% of the Discount Rate, basing on one-year average on the inflation rate assessment.

Figure 5 shows the MES profitability index calculated for different TDS and Market Scenarios (Present and Future). Under the Current TDS and Present Market conditions, the MES operating as Peaker or Ancillary, is not economically sustainable (profitability index<1).

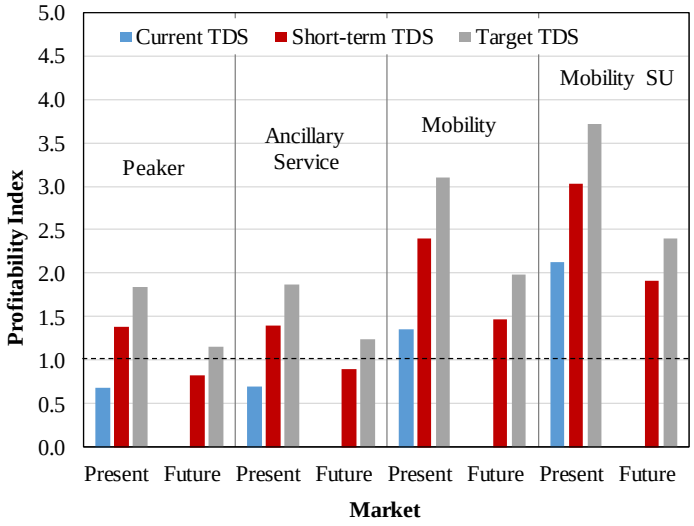

Figure 5. MES Profitability Index vs TDS for different Energy Vectors Market Scenarios

These management strategies are always (in PM and FM) profitable in the Target TDS; on the contrary, in the Shot-Term TDS they are profitable only in the PM.

The Mobility management strategies result always profitable thanks to the highest prices of hydrogen with respect to the electricity ones. In the Current TDS and Present Market, the Mobility management strategy allows to obtain a Net Present Value, an Internal Rate of Return and a Discounted Payback Period equal to 1.6 M€, 4% and 15.2 years, respectively, for the MES configuration, and 3.5 M€, 11% and 9.5 years, respectively for the MES-SU one.

In table 17 the MES economic performances in the Short-Term TDS and Target TDS are illustrated.

Table 17. Economic performance under Short-term TDS and Target TDS and under Present and Future Market scenarios

Technology Development Scenario	Economic Parameters	Present Market				Future Market			
		Management Strategies							
		Peaker	Ancillary Service	Mobility	Mobility SU	Peaker	Ancillary Service	Mobility	Mobility SU
Short-term TDS	Profitability Index	1.4	1.4	2.4	3.0	0.8	0.9	1.5	1.9
	NPV (k€)	1112.4	1180.7	4134.0	4927.8	-	-	1408.8	2202.6
	IRR (%)	4.7	4.9	12.6	16.8	-	-	5.5	9.0
	DPBP (years)	14.8	14.6	8.4	6.8	-	-	13.8	10.6
Target TDS	Profitability Index	1.8	1.9	3.1	3.7	1.2	1.2	2.0	2.4
	NPV (k€)	1999.5	2067.9	5021.1	5532.0	374.4	586.4	2329.3	2840.3
	IRR (%)	8.6	8.8	17.7	21.4	2.6	3.5	9.7	12.6
	DPBP (years)	11.1	10.8	6.5	5.6	17.7	16.4	9.9	8.4

On the Short-term/Target TDSs, the Peaker and the Ancillary Service management strategies, more focused on the electrical production, can allow to reach the economic sustainability of the MES only in the Present Market, whereas, in the Future Market, they are slightly convenient just for the Target TDS (profitability index greater than 1).

Furthermore, by analyzing the Profitability index and the NPV and DPBP indicators, it is clear that the hydrogen production is the main contributor to the MES economic sustainability: in the mobility management strategies (MES and MES-SU configurations) these parameters are much better than those obtained in the Peaker and Ancillary Service strategies, both in the Short-term TDS and Target TDS.

Finally, for the Mobility and Mobility SU management strategies, the decrease of the hydrogen price (8 €/kg vs 11 €/kg) causes the reduction of the profitability in the Target TDS.

The best solution is achieved in the Present Market and under Target TDS (3.7 and 5.6 years for the Profitability index and DPBP, respectively).

6. Concluding Remarks

In this study a biomass-based Multi-Energy System (MES) for the combined hydrogen, heat and electricity is designed and analyzed from energy and economic points of view.

The energy analysis has been conducted by using the numerical modeling based on thermo-electrochemical sub-models properly developed by using a commercial software. The system behavior has been investigated by varying the SOFC electric load from 100% to 30% that means full electricity production and maximum hydrogen production, respectively (the minimum load that permits to sustain the electric power consumption of the hydrogen separation and compression units).

Modeling results show that the polygeneration system permits to achieve a CFP efficiency ranging from a minimum value of 68.5% (at 80% SOFC load) to a maximum value of 72.3%, reached at the minimum SOFC load (30%), even if the calculated energy saving results to be higher when the SOFC power unit works at rated power (100% load).

Results of the energy analysis have been used to perform the economic assessment based on some financial parameters (Net Present Value, Pay-back Period, Profitability Index). By taking into account the electricity, heat and hydrogen markets in different pricing scenarios, 4 management strategies have been investigated and analyzed.

Results show that, under Present and Future Market scenarios, the hydrogen production is the main contributor to the MES economic sustainability and the use of the MES within a Virtual Power Plant (option useful for increasing the grid resilience), is less convenient in comparison to the MES managed for the hydrogen production (Mobility strategies).

Thus, the biogas polygeneration system, as the core of the proposed MES, can represent an alternative solution to operate existing biogas power plants (based on anaerobic digestion process) when, in the near future, incentives in the electric power production will no longer be available.

REFERENCES

1. Jana K, Ray A, Majoumerd MM, , Assadi M, De S. Polygeneration as a future sustainable energy solution – A comprehensive review. Applied Energy 2017; 201:88-111.

2. Bracco S, Delfino F, Pampararo F, Robba M, Rossi M. Dynamic optimization-based architecture for polygeneration microgrids with tri-generation, renewables, storage systems and electrical vehicles. Energy Conversion and Management 2015, 96:511–520

3. Ferrari ML, Traverso A, Massardo AF. Smart polygeneration grids: Experimental performance curves of different prime movers. Applied Energy 2016:162;622-630.

4. Ghaem Sigarchian S, Malmquist A, Martin V. The choice of operating strategy for a complex polygeneration system: A case study for a residential building in Italy. Energy Conversion and Management 2018;163: 278-291

5. Facci, A.L., Cigolotti, V., Jannelli, E., Ubertini, S. "Technical and economic assessment of a SOFC-based energy system for combined cooling, heating and power" (2017) Applied Energy, Vol. 192, pp. 563-574

6. Rivarolo M, Cuneo A, Traverso A, Massardo AF. Design optimisation of smart poly-generation energy districts through a model-based approach. Applied Thermal Engineering 2016; 99:291-301

7. Rostamzadeh H, Gargari SG, Namin AS, Ghaebi H. A novel multigeneration system driven by a hybrid biogas-geothermal heat source, Part I: Thermodynamic modeling. Energy Conversion and Management. 2018;177:535-62.

8. Spencer JD, Moton JM, Gibbons WT, Gluesenkamp K, Ahmed II, Taverner AM, McGahagan D, Tesfaye M, Gupta C, Bourne RP, Monje V, Gregory S. Jackson GS. Design of a combined heat, hydrogen, and power plant from university campus waste streams. International Journal of Hydrogen Energy. 2013;38:4889-4900.

9. Perna A, Minutillo M, Jannelli E, Cigolotti V, Nam SW, Han J. Design and performance assessment of a combined heat, hydrogen and power (CHHP) system based on ammonia-fueled SOFC, Applied Energy 2018;231: 1216-1229

10. B. Wu, X. Zhang, D. Shang, D. Bao, S. Zhang, T. Zheng, "Energetic-environmental-economic assessment of the biogas system with three utilization pathways: combined heat and power, biomethane and fuel cell" (2016) Bioresour. Technol., Vol. 214, pp. 722-728, ISSN 0960-8524

11. de Jong, E.; Jungmeier, G., Biorefinery concepts in comparison to petrochemical refineries. Industrial Biorefineries & White Biotechnology 2015, 3-33

12. Ghatak HR, Biorefineries from the perspective of sustainability: Feedstocks, products, and processes, Renewable and Sustainable Energy Reviews. 2011;15 (8):4042-52,

13. Demirbas A. Biofuels sources, biofuel policy, biofuel economy and global biofuel projections, Energy Conversion and Management 2008; 49: 2106–2116

14. Mohsen R, Mehrpooya M. Investigation of a new integrated biofuel production process via fast pyrolysis, co-gasification and hydro up grading. Energy Conversion and Management 2018;161: 35-52.

15. Tribioli L, Cozzolino R, Barbieri M, Optimal control of a repowered vehicle: plug-in fuel cell against plug-in hybrid electric powertrain. 2015 American Institute of Physics, Vol. 1648.

16. Ferrari ML, Rivarolo M, Massardo AF. Hydrogen production system from photovoltaic panels: experimental characterization and size optimization. Energy Conversion and Management 2016; 116:194-202.

17. Scarlat N, Dallemand JF, Fahl F. Biogas: Developments and perspectives in Europe. Renewable Energy 2018;129:457-472

18. Pablo-Romero M, Sánchez-Braza A, Salvador-Ponce J, Sánchez-Labrador N. An overview of feed-in tariffs, premiums and tenders to promote electricity from biogas in the EU-28, Renewable and Sustainable Energy Reviews. 2017;73:1366-79.

19. Ma LC, Castro-Dominguez B, Kazantzis NK, Ma YH. Economic performance evaluation of process system design flexibility options under uncertainty: The case of hydrogen production plants with integrated membrane technology and CO2 capture. Computers & Chemical Engineering 2017;99:214-229

20. Ranieri L, Mossa G, Pellegrino R, Digiesi S. Energy Recovery from the Organic Fraction of Municipal Solid Waste: A Real Options-Based Facility Assessment. Sustainability 2018;10:368

21. Perna A. Theoretical analysis on the autothermal reforming process of ethanol as fuel for a proton exchange membrane fuel cell system. Journal of Fuel Cell Science and Technology 2007; 4 (4):468-473

22. Palma V, Ricca A, Addeo B, Rea M, Paolillo G. Hydrogen production in a compact ATR-based KW-scale fuel processor. Proceedings of the 6th European Fuel Cell - Piero Lunghi Conference, EFC 2015;165-166

23. Palma V, Ricca A, Ciambelli P. Fuel cell feed system based on H2 production by a compact multi-fuel catalytic ATR reactor. International Journal of Hydrogen Energy. 2013;38:406-16.

24. Montenegro Camacho YS, Bensaid S, Lorentzou S, Vlachos N, Pantoleontos G, Konstandopoulos A, Luneau M, Meunier FC, Guilhaume N, Schuurman Y, Werzner E, Herrmann A, Rau A, Krause H, Rezaei E, Ortona A, Gianella S, Khinsky A, Antonini M, Marchisio L, Vilardo F, Trimis D, Fino D. Development of a robust and efficient biogas processor for hydrogen production. Part 1: Modelling and simulation. International Journal of Hydrogen Energy. 2017;42:22841-55

25. Yin H, Yip AC. A review on the production and purification of biomass-derived hydrogen using emerging membrane technologies. Catalysts 2017;7(10):297

26. https://www.aspentech.com/en/products/engineering/aspen-plus

27. Perna A, Minutillo M, Jannelli E, Cigolotti V, Nam SW, Sung PY. Performance assessment of a hybrid SOFC-MGT cogeneration power plant fed by syngas from a biomass down-draft gasifier. Applied Energy 2018;227: 80-91

28. Perna A, Minutillo M, Jannelli E. Designing and analyzing an electric energy storage system based on reversible solid oxide cells. Energy Conversion and Management 2018;159:381-95

29. Rahimpour MR, Samimi F, Babapoor A, Tohidian T, Mohebi S. Palladium membranes applications in reaction systems for hydrogen separation and purification: A review. Chemical Engineering and Processing: Process Intensification 2017;121: 24-49

30. Alique D, Martinez-Diaz D, Sanz R, Calles JA. Review of Supported Pd-Based Membranes Preparation by Electroless Plating for Ultra-Pure Hydrogen Production. Membranes 2018; 8(1):5

31. Gallucci F, Medrano J, Fernandez E, Melendez J, van Sint Annaland M, Pacheco A. Advances on High Temperature Pd-Based Membranes and Membrane Reactors for Hydrogen Purifcation and Production. Journal of Membrane Science and Research 2017;3(3):142-156

32. Perna A, Cicconardi SP, Cozzolino R. Performance evaluation of a fuel processing system based on membrane reactors technology integrated with a PEMFC stack. International Journal of Hydrogen Energy 2011;36(16):9906-15

33. Linde. Hydrogen technologies. The Ionic Compressor 90 MPa – IC90. Technical brochure; 2015

34. Linde. Linde's innovative technologies for the hydrogen infrastructure. 2015

35. Mayer M. From prototype to serial production: Manufacturing hydrogen fuelling stations. A3PS Ecomobility Conference, 20 October 2014, Vienna, Austria.

36. Van de Ven JD, Li PY. Liquid piston gas compression. Applied Energy 2009; 86(10):2183-91

37. Commission Delegated Regulation (EU) 2015-2402 Of 12 October 2015, https:--eur-lex.europa.eu-legal-content-IT-TXT-?uri=CELEX%3A32015R2402

38. Perna A, Minutillo M, Jannelli E. Hydrogen from intermittent renewable energy sources as gasification medium in integrated waste gasification combined cycle power plants: a performance comparison. Energy 2016;94:457-465

39. Y. Parag and B. K. Sovacool, "Electricity market design for the prosumer era", Nature Energy, 16032 (2016).

40. Adam Hirsch, Yael Parag, Josep Guerrero, Microgrids: A review of technologies, key drivers, and outstanding issues, Renewable and Sustainable Energy Reviews. 2018;90: 402-411.

41. A. Bidram, A. Davoudi, F. L. Lewis and Z. Qu, Secondary control of microgrids based on distributed cooperative control of multi-agent systems, in IET Generation, Transmission & Distribution, vol. 7, no. 8, pp. 822-831, Aug. 2013. doi: 10.1049/iet-gtd.2012.0576.

42. Provisional data on operation of the Italian electricity system 2017; http://www.terna.it/en-gb/sistemaelettrico/dispacciamento/datiesercizio/datiprovvisoridesercizio.aspx

43. Arun K.S. Iyengar, Richard A. Newby, Dale L. Keairns, Techno-Economic Analysis of Integrated Gasification Fuel Cell Systems Created by Energy Sector Planning and Analysis for SEAP & OPPB, November 24, 2014, DOE-NETL- 341-112613

44. Cuneo A, Zaccaria V, Tucker D, Sorce A. Gas turbine size optimization in a hybrid system considering SOFC degradation. Applied Energy 2018; 230:855-864

45. Giarola S., Forte O., Lanzini R., Gandiglio M., Santarelli M., Hawkes A., Techno-economic assessment of biogas-fed solid oxide fuel cell combined heat and power system at industrial scale, Applied Energy 2018;211:689–704

46. Ammermann H, Hoff P, Atanasiu M, Aylor J, Kaufmann M, Tisler O. Advancing Europe's energy systems: stationary fuel cells in distributed generation. Technical report. Fuel Cells and Hydrogen Joint Undertaking; 2015

47. Fuel Cells and Hydrogen2 Joint Undertaking. Addendum to the Multi-Annual Work Plan 2014-2020. www.fch.europa.eu/news/fuel-cells-and-hydrogen-2-joint-undertaking

48. The international council on clean transportation, Developing hydrogen fueling infrastructure for fuel cell vehicles: A status update, OCTOBER 2017